Oxygen impurities in NiAl: Relaxation effects

David Djajaputra and Bernard R. Cooper
Department of Physics, West Virginia University, P. O. Box 6315, Morgantown, West Virginia 26506
(Received 26 March 2001; published 8 August 2001)

We have used a full-potential linear muffin-tin orbital method to calculate the effects of oxygen impurities on the electronic structure of NiAl. Using the supercell method with a 16-atom supercell we have investigated the cases where an oxygen atom is substitutionally placed at either a nickel or an aluminum site. Full relaxation of the atoms within the supercell was allowed. We found that oxygen prefers to occupy a nickel site over an aluminum site with a site selection energy of 138 mRy (21 370 K). An oxygen atom placed at an aluminum site is found to cause a substantial relaxation of its nickel neighbors *away* from it. In contrast, this steric repulsion is hardly present when the oxygen atom occupies the nickel site and is surrounded by aluminum neighbors. We comment on the possible relation of this effect to the pesting degradation phenomenon (essentially spontaneous disintegration in air) in nickel aluminides.

DOI: 10.1103/PhysRevB.64.085121 PACS number(s): 71.55.Ak, 71.15.Nc, 71.20.Lp

Nickel aluminides are potentially important industrial alloys in high-temperature structural applications, such as gas turbine engines, because they possess many desired physical properties. Among these are their low density, high strength, and good thermal conductivity, the last being an important factor in dissipating the heat generated by the engines. The great interest in these alloys has resulted in a large body of literature.[1–6]

Many properties of NiAl have been intensely investigated using various computational electronic structure methods. The band structure of NiAl has been experimentally studied using photoemission and calculated using the linear augmented Slater-type orbital method by Lui *et al.*[7] They found that NiAl behaves like a good itinerant metal: the self-energy corrections in NiAl are significantly less than in pure ferromagnetic nickel. Band structure results should therefore provide a good description of the electronic properties of NiAl. Kim *et al.*[8] also calculated the band structure of NiAl using a semirelativistic linearized augmented plane wave method and compared the result with the experimental optical spectra.[8,9] Their result agreed with the result of Lui *et al.*, and they found no need to incorporate self-energy corrections into the spectrum in order to fit their experimental data. This is markedly different from the result for CoAl where the corrections are needed to make a good fit.[8] One can therefore put some confidence in the band structure results for NiAl.

Most research on nickel aluminides has been devoted to the effort to understand the complex effects of impurities and other kinds of crystal defect.[10] Uses of nickel aluminides, especially in polycrystalline form, as structural materials are limited by their brittleness at high temperature (over 800 °C) where they become prone to brittle intergranular fracture and by their low ductility at intermediate temperatures. Certain additive impurities have been found to greatly improve the room-temperature intergranular cohesion and the tensile ductility. The most notable of these cohesion enhancers is boron[11] which can improve the tensile ductility by an order of magnitude and change the fracture mode from intergranular to transgranular.[10] Sun *et al.*[12] have studied the effects of boron and hydrogen on the cohesion of Ni_3Al using a full-potential linear muffin-tin orbital (FP-LMTO) method. They concluded that boron improves the local cohesion by reducing the bonding charge directionality around the nickel atoms and by inducing an increase of the interstitial bonding charge.

At intermediate to high temperature, nickel aluminides, and many other intermetallics, exhibit brittle intergranular fracture due to the oxygen-induced embrittlement.[10] At high temperature, the oxidation will selectively attack the least noble constituent, which is aluminum, and form the oxide product Al_2O_3.[14] In some cases, these oxide products can provide a stable oxide layer that protects the alloy underneath it from further oxygen attack. NiAl is one of the intermetallics that are able to form a protective oxide layer and therefore is used as a coating for other intermetallic alloys.[13]

The oxidation resistance decreases as we move toward the nickel-rich part of the Ni-Al phase diagram. The most damaging effect of oxygen occurs when it causes the pesting degradation phenomenon (essentially spontaneous disintegration in air). Some intermetallic compounds that form protective coatings at high temperature literally disintegrate when heated in the intermediate temperature range.[13,14] This occurs only on polycrystalline samples, so it is sometimes also termed intergranular attack.[13] Among nickel aluminides, the pesting phenomenon has been observed in NiAl,[14,15] and in Ni_3Al.[16]

Despite the extreme effects that it can cause, we are unaware of any previous *ab initio* study performed on the effects of oxygen in nickel aluminides. Moreover, most studies of other impurities are limited by not allowing the atoms within the supercell to relax. Relaxation effects are especially relevant to the case of impurity atoms located at the grain boundary where they can be relatively free to move and bond to certain constituent atoms of the host alloy.

In this work we have used a full-potential linear muffin-tin orbital method within the local density approximation (LDA) to study the effects of oxygen impurities on the electronic structure of NiAl. The details of this method have been documented elsewhere.[17–19] For the work reported in this paper, we use nine (spd) orbitals for each atom in the supercell and assign three LMTO basis functions for each orbital, corresponding to $\kappa = -1.50, -0.50$, and 1.00, respec-

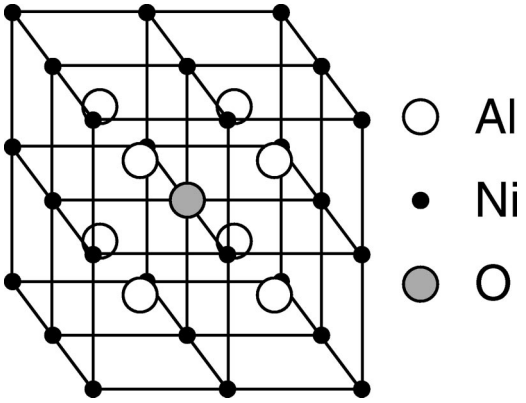

FIG. 1. The 16-atom supercell used in the present work. The cubic supercell is built up from 2^3 unit cells of NiAl. The impurity atom (O) is placed at the center of the supercell, substituting for Ni in this picture (supercell Ni_7Al_8O). We also use a similar supercell, where the oxygen atom is placed at an Al site (supercell Ni_8Al_7O).

tively. Here κ is the wave-number parameter; the square of κ is the absolute value of the energy of the basis function, measured relative to the muffin-tin zero, while its sign is equal to the sign of the energy.[20] The large number of basis functions used provides our full-potential method with good flexibility to find the lowest-energy density.

The 16-atom supercell that was used in the computation is shown in Fig. 1. Pure NiAl crystallizes in the $B2$ structure with lattice constant of 5.4450 a.u.[21] The calculated equilibrium lattice constant using our FP-LMTO method is 5.3451 a.u., which agrees with the experimental value within 2%. The supercell is constructed from 2^3 unit cells of NiAl. The oxygen impurity atom is placed at the center of the supercell, replacing a nickel or an aluminum atom. For a given supercell lattice constant, we allow the atoms in the unit cell to relax to find the minimum total energy for that lattice constant. By symmetry, only the eight nearest neighbors of the oxygen atom are allowed to relax, and they can only move radially away or toward the center oxygen atom (we do not consider the possibility of symmetry breaking). Only one parameter is needed to describe the relaxation, namely, the distance of these neighboring atoms from the central oxygen atom.

The computed total energies for the relaxed 16-atom supercell are shown in Fig. 2 and compared with the curves for the unrelaxed supercell. Each continuous curve shown in Fig. 2 is obtained by fitting 8–9 LMTO data points computed around the minimum-energy lattice constant using an eight-parameter fitting function. The calculated relaxation energies E_R are listed in Table I. We use the following definition for the relaxation energy:

$$E_R = E_r(a_r) - E_u(a_u), \tag{1}$$

with a_u and a_r being the lattice constants that give the minimum energy for the unrelaxed (E_u) and relaxed (E_r) configurations, respectively. The computed energy curves lie very close to each other, and the relaxation energies are relatively small, being about 100 K and 200 K (in equivalent temperature scale) for oxygen at the Al and Ni sites, respectively. These numbers are about the same as the accuracy of the LMTO-LDA method, which has been estimated at about 1 mRy (158 K).[22] Numerically, however, our FP-LMTO method did not produce any notable fluctuation and we believe that some confidence can be placed in these numbers.

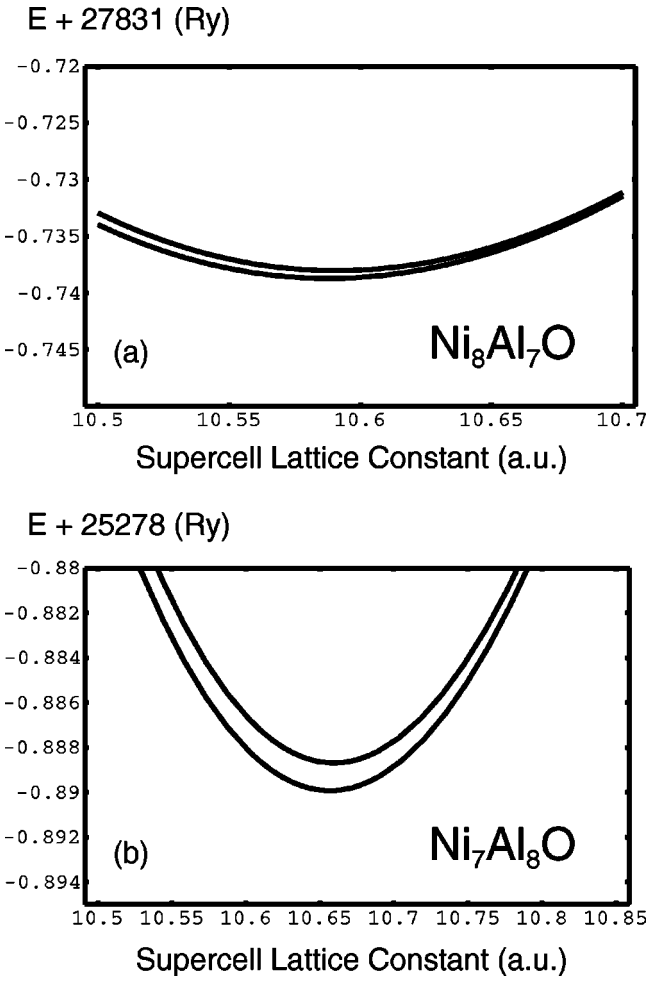

FIG. 2. The FP-LMTO total energy with 16-atom supercell for the case of oxygen substituting for an aluminum atom (a), and oxygen substituting for a nickel atom (b). In both panels, the top curve is for an unrelaxed supercell while the bottom curve is for the relaxed supercell. The equilibrium lattice spacing and the relaxation energy are listed in Table I.

The computed relaxation data are shown in Fig. 3 where we track the nearest-neighbor distances between the atoms in the unit cell on the (011) plane as we change the supercell lattice constant. Figure 3(b) displays the results for the case of oxygen at the Ni site. Shown are d(Al-O), which is the

TABLE I. Equilibrium lattice constant a_r for fully relaxed supercell, its total energy E_r, and the corresponding relaxation energy E_R (relative to the unrelaxed supercell).

Supercell	a_r (a.u.)	E_r (Ry)	E_R (mRy)
Ni_8Al_7O	10.5878	−27 831.7387	−0.675
Ni_7Al_8O	10.6567	−25 278.8899	−1.236

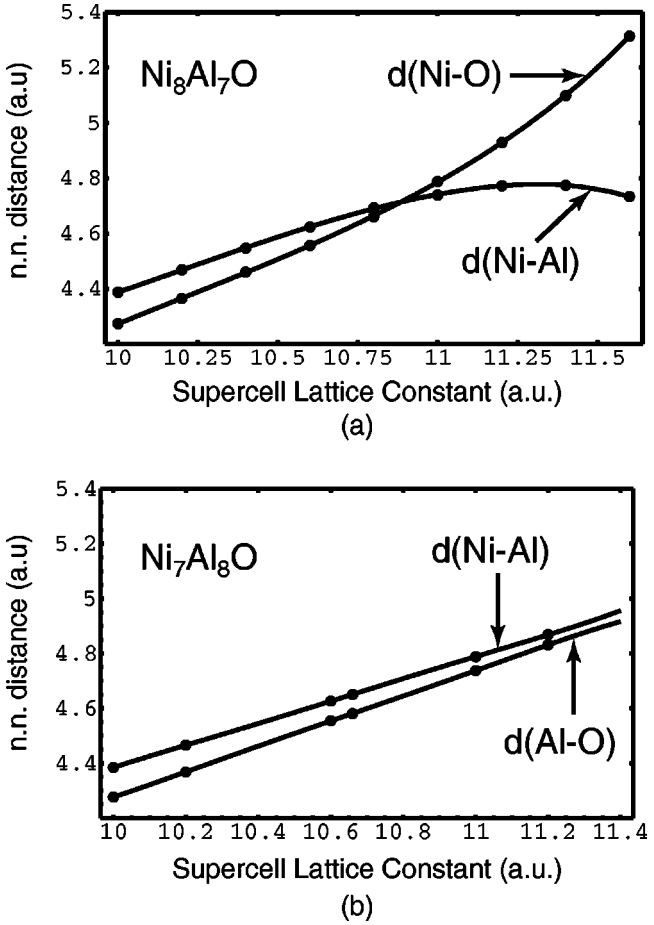

FIG. 3. Nearest-neighbor (*NN*) distances between atoms in the unit cell on the (011) plane as a function of the supercell lattice constant. (a) Oxygen at Al site. For small lattice constants the movement of the Ni atoms is toward the central oxygen atom and away from the corner Al atoms. At large lattice constants the direction of movement reverses: the Ni atoms are displaced significantly closer to the corner Al atoms. This presumably reflects a steric repulsion between oxygen and nickel in the NiAl environment. (b) Oxygen at Ni site. Apparently, the Al atoms are attracted about equally strongly by the O and the Ni atoms. This results in small relaxation.

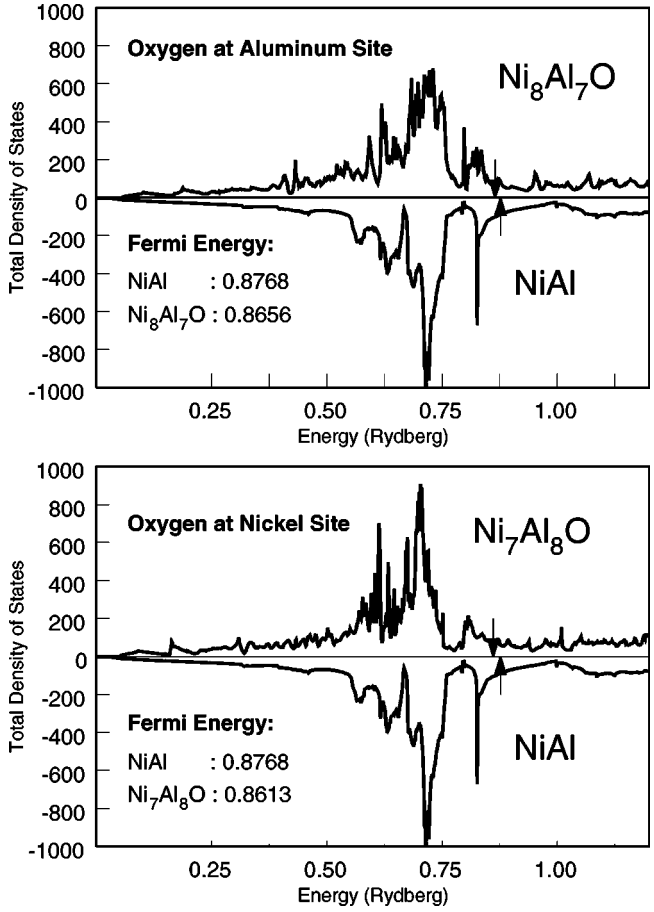

FIG. 4. Total density of states for the 16-atom supercell calculated using the FP-LMTO method. For comparison, in each panel we also show the negative of the density of states for pure NiAl. Vertical arrows on the energy axis point to the positions of the Fermi energy. (a) Oxygen at Al site. (b) Oxygen at Ni site.

distance between the central O atom and one of its eight nearest-neighbor Al atoms, and $d(\text{Ni-Al})$, which is the distance between the Al atom and its nearest-neighbor Ni atom (at one of the corners of the supercell). Without relaxation, the oxygen atom will be at $(0,0,0)$, the aluminum atom at, e.g., $(\frac{1}{4},\frac{1}{4},\frac{1}{4})$, and the nickel atom at $(\frac{1}{2},\frac{1}{2},\frac{1}{2})$. As we vary the lattice constant a, the distances scale linearly with it: $d(\text{Al-O}) = d(\text{Ni-Al}) = a\sqrt{3}/4$. This relation is still approximately followed when we relax the atoms, as shown in Fig. 3, with the aluminum atoms only attracted slightly more toward the central oxygen atom.

A significantly different situation occurs if we place the oxygen atom at the Al site, as shown in Fig. 3(a). In this case, the nearest neighbors of the central O atom are Ni atoms, the distance between them is $d(\text{Ni-O})$, and each of these Ni atoms neighbors an Al atom at its nearest corner of the supercell, where the distance between them is denoted by $d(\text{Ni-Al})$. Under pressure, for lattice constants smaller than the equilibrium value, the Ni atoms slightly relax toward the central oxygen atom, away from the corner Al atoms. However, as the lattice constant is increased above the equilibrium value, the intervening Ni atoms very quickly start to move *away* from the central oxygen atom and relax closer to their neighboring Al atoms. We view this as reflecting a mutual repulsion between the oxygen and nickel atoms in the NiAl environment. Experimentally, the formation rate of aluminum oxide during exposure of nickel aluminides to oxygen is known to be much higher than that of nickel oxide.[13,14]

The relaxation behavior of the atoms is thus seen to differ markedly depending on whether the impurity oxygen atom occupies an Al or a Ni site, especially in the stretched-supercell case, where the atoms have greater freedom to move around. This may have some relevance to the case of oxygen attack on polycrystalline nickel aluminides (pesting). We believe this reflects a situation where the oxygen atoms cause a sort of ''wedge effect,'' seeping into the grain boundaries to reduce the intergranular cohesion and opening up the polycrystal wider for more infiltration of oxygen. This pro-

vides a *self-propelling* mechanism for oxygen atoms to infiltrate a polycrystal of nickel aluminide and, along the way, destroy the intergranular cohesion between the grains, effectively disintegrating the polycrystal. In this scenario the pesting phenomenon can be seen to be fueled by the *combination* of two major factors: the thermal intergranular diffusion of oxygen and the strongly *preferential* bonding of oxygen with one of the components of the alloy (aluminum in nickel aluminides). More insights into this phenomenon can perhaps be obtained by performing a molecular-dynamics (MD) simulation using microscopic parameters that are extracted from an *ab initio* calculation such as reported in this paper. Campbell *et al.* have performed such a MD simulation for the oxidation of aluminum nanoclusters.[23]

The energetics of the preferential bonding of oxygen in NiAl can be studied by calculating the site selection energy.[24] The total energy for pure bulk metal (per atom) is used to provide a reference energy for the constituent species. In our case, these are the total energies of fcc Ni and fcc Al. These have been calculated using the same FP-LMTO method and their values are

$$E(\mathrm{Ni}) = -3036.8304 \ \ \mathrm{Ry}, \tag{2}$$

$$E(\mathrm{Al}) = -483.8440 \ \ \mathrm{Ry}. \tag{3}$$

The total energies for the 16-atom supercell with one oxygen atom replacing a Ni or an Al atom are listed in Table I. We list the minimum of the total energy of the relaxed supercell. The site selection energy is defined to be the difference between the following two values:[24]

$$E_{\mathrm{Ni}} = E(\mathrm{Ni}) + E(\mathrm{Ni_7Al_8O}) = -28\,315.7204 \ \ \mathrm{Ry}, \tag{4}$$

$$E_{\mathrm{Al}} = E(\mathrm{Al}) + E(\mathrm{Ni_8Al_7O}) = -28\,315.5827 \ \ \mathrm{Ry}. \tag{5}$$

Taking the difference, an oxygen atom in NiAl will prefer to occupy a nickel site with the site selection energy of

$$\Delta E = 137.7 \ \ \mathrm{mRy} = 21\,730 \ \ \mathrm{K}. \tag{6}$$

That oxygen will prefer to occupy a nickel site over an aluminum site seems to contradict one's expectation based on the atomic radii of the constituent atoms. Since the atomic radius of oxygen is closer to that of aluminum rather than nickel, one would expect that the oxygen would prefer to occupy an aluminum site over the nickel site. To understand our result, we need to recall the previously deduced mutual repulsion between oxygen and nickel in the NiAl environment. An oxygen atom will therefore prefer to be surrounded by nearest neighbors of aluminum, rather than nickel, atoms. It will achieve this simply by occupying a nickel site.

Finally, in Fig. 4 we show the total density of states (DOS) for the two supercell systems that we study in this work, Ni_8Al_7O and Ni_7Al_8O, calculated from the FP-LMTO energy bands using the tetrahedron method. For comparison, we also show the corresponding total DOS for pure NiAl. The dominant feature of the NiAl DOS is the existence of the sharp peaks due to the *d* orbitals of nickel, which hybridize only weakly with the other orbitals. Placing the oxygen atom at the Al site in Ni_8Al_7O allows for some hybridization between these *d* orbitals and the delocalized *p* orbitals of oxygen. This results in reduced sharpness of the Ni *d* state peaks in the DOS without essentially any shift in the position of the peaks, as can be seen in Fig. 4(a). On the other hand, if we place the oxygen impurity at the Ni site, then the nickel atoms will not have the oxygen atom as their nearest neighbor. The oxygen atom will have the aluminum atoms as its nearest neighbors. Being the more electronegative element, oxygen will interact with the valence electrons of Al and will localize a portion of those electrons around itself. This depletes the Ni sites of some of the electrons from the Al that was formerly occupying its site in the pure NiAl case. The end result of this is a lower electrostatic potential at the Ni sites and the reduction of the on-site energies of the *d* orbitals of Ni, without much change in their spatial extent. This translates to an almost rigid downward shift in the position of the Ni *d* state peaks in the DOS without much alteration in their width. This downward shift of about 25 mRy can quite readily be discerned in Fig. 4(b).

This work benefited from much discussion with our late colleague David L. Price. A large part of the computational work for this project was performed at the Maui High Performance Computing Center (MHPCC). This work was supported by AF-OSR Grant No. F49620-99-1-0274.

[1] R. Darolia, JOM **43**, 44 (1991).

[2] *International Symposium on Nickel and Iron Aluminides: Processing, Properties, and Applications*, edited by S.C. Deevi *et al.* (ASM International, Materials Park, OH, 1997).

[3] D.B. Miracle, Acta Metall. Mater. **41**, 649 (1993).

[4] *Intermetallic Compounds: Principles and Practice*, edited by J. H. Westbrook and R.L. Fleischer (John Wiley and Sons, Chichester, England, 1995), Vol. 2.

[5] C.T. Liu and D.P. Pope, in *Intermetallic Compounds: Principles and Practice* (Ref. 4), pp. 17–51.

[6] D.B. Miracle and R. Darolia, in *Intermetallic Compounds: Principles and Practice* (Ref. 4), pp. 53–72.

[7] S.C. Lui, J.W. Davenport, E.W. Plummer, D.M. Zehner, and G.W. Fernando, Phys. Rev. B **42**, 1582 (1990).

[8] K.J. Kim, B.N. Harmon, and D.W. Lynch, Phys. Rev. B **43**, 1948 (1991).

[9] K. Schlemper and L.K. Thomas, Phys. Rev. B **50**, 17 802 (1994).

[10] C. T. Liu and E. P. George, in *International Symposium on Nickel and Iron Aluminides: Processing, Properties, and Applications* (Ref. 2), pp. 21–31.

[11] K. Aoki and O. Izumi, Nippon Kinzoku Gakkaishi **43**, 1190 (1979).

[12] S.N. Sun, N. Kioussis, S.P. Lim, A. Gonis, and W.H. Gourdin, Phys. Rev. B **52**, 14 421 (1995).

[13] J. Doychak, in *Intermetallic Compounds: Principles and Practice*, edited by J. H. Westbrook and R. L. Fleischer (John Wiley

and Sons, Chichester, England, 1995), Vol. 1, pp. 977–1016.
[14] E.A. Aitken, in *Intermetallic Compounds*, edited by J. H. Westbrook (John Wiley and Sons, New York, 1966), pp. 491–516.
[15] J.H. Westbrook and D.L. Wood, J. Nucl. Mater. **12**, 208 (1964).
[16] T.H. Chuang, Y.C. Pan, and S.E. Hsu, Metall. Trans. A **22**, 1801 (1991).
[17] D.L. Price and B.R. Cooper, Phys. Rev. B **39**, 4945 (1989).
[18] D.L. Price, J.M. Wills, and B.R. Cooper, Phys. Rev. B **46**, 11 368 (1992).
[19] J. M. Wills, O. Eriksson, M. Alouani, and D. L. Price, in *Electronic Structure and Physical Properties of Solids*, edited by H. Dreyssé (Springer-Verlag, Berlin, 2000), pp. 148–167.
[20] H. L. Skriver, *The LMTO Method* (Springer-Verlag, Berlin, 1984), Chap. 5.
[21] W. B. Pearson, *Handbook of Lattice Spacings and Structures of Metals and Alloys* (Pergamon, New York, 1958).
[22] U. von Barth, *Lectures on Methods of Electronic Structure Calculations* (World Scientific, Singapore, 1994), pp. 21–62.
[23] T. Campbell, R.K. Kalia, A. Nakano, P. Vashishta, S. Ogata, and S. Rodgers, Phys. Rev. Lett. **82**, 4866 (1999).
[24] P.K. Khowash, D.L. Price, and B.R. Cooper, Phys. Rev. B **47**, 9884 (1993).